Dto. de Ingeniería Eléctrica y de Computadoras
Universidad Nacional del Sur

DIEC

An introduction to cellular IoT: Signal processing aspects of NB-IoT

Juan Cousseau (jcousseau@uns.edu.ar)
Laboratorio de Procesamiento de Señales y Comunicaciones
Instituto de Investigaciones en Ingeniería Eléctrica - CONICET

NEON
Network of Competence on Internet of Things
Co-funded by the Erasmus+ Programme of the European Union

Dto. de Ingeniería Eléctrica y de Computadoras
Universidad Nacional del Sur

Outline

Introduction – motivation

IoT applications and challenges

IoT proprietary (LoRa) and/or licensed solutions (NB-IoT)

OFDM

OFDM system- Discrete model – Spectral efficiency – Characteristics

OFDM Sensitivity to synchronization errors.

Downlink time and CFO synchronization

3GPP LTE Characteristics

Network architecture

LTE layer functions

Physical channel characteristics

Congestion control and power efficiency

NB-IoT basics

Physical Layer numerology - Design Principles

DL and UL Physical Channels and Signals

Orthogonal frequency division multiplexing OFDM

- OFDM system: Discrete model – Spectral efficiency – Characteristics
- OFDM based multiple access schemes
- OFDM sensitivity to synchronization errors

OFDM system

Main idea: to divide a high rate data stream into Nu orthogonal carriers, using an N-point IDFT (N > Nu).

Result: high complexity linear equalization required for a frequency selective channel can be replaced by a set of one-tap complex equalizers.

Due to channel time dispersion, contiguous blocks may overlap producing IBI. Then, introduction of the cyclic prefix.

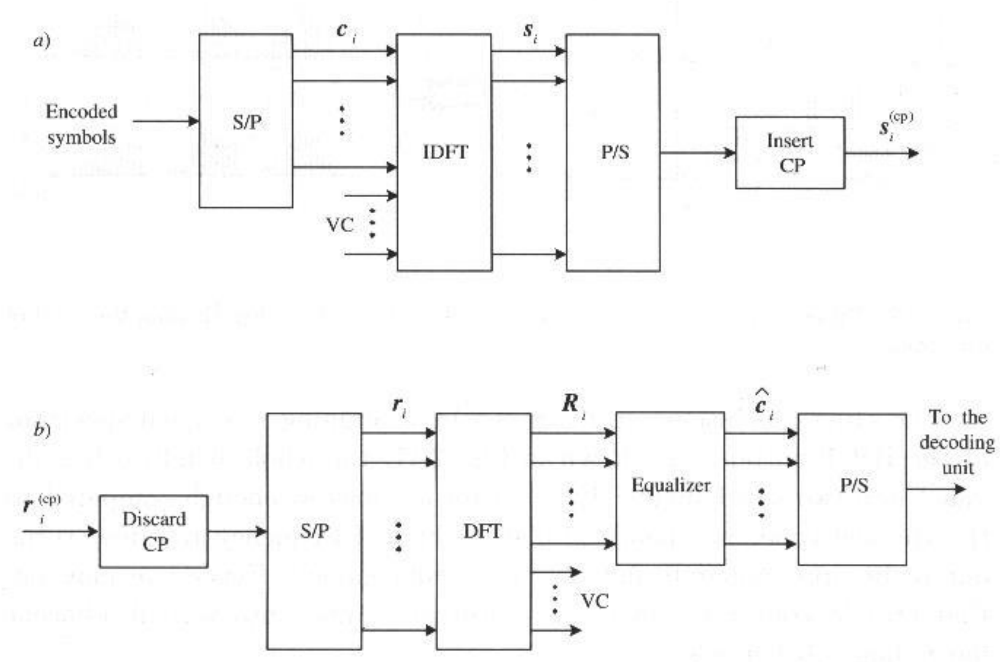

Fig. 2.15 Block diagram of a typical OFDM system: a) transmitter; b) receiver.

OFDM system

$$\boldsymbol{s}_i = \boldsymbol{F}^H \boldsymbol{c}_i \qquad [\boldsymbol{F}]_{n,k} = \frac{1}{\sqrt{N}} \exp\left(\frac{-j2\pi nk}{N}\right)$$

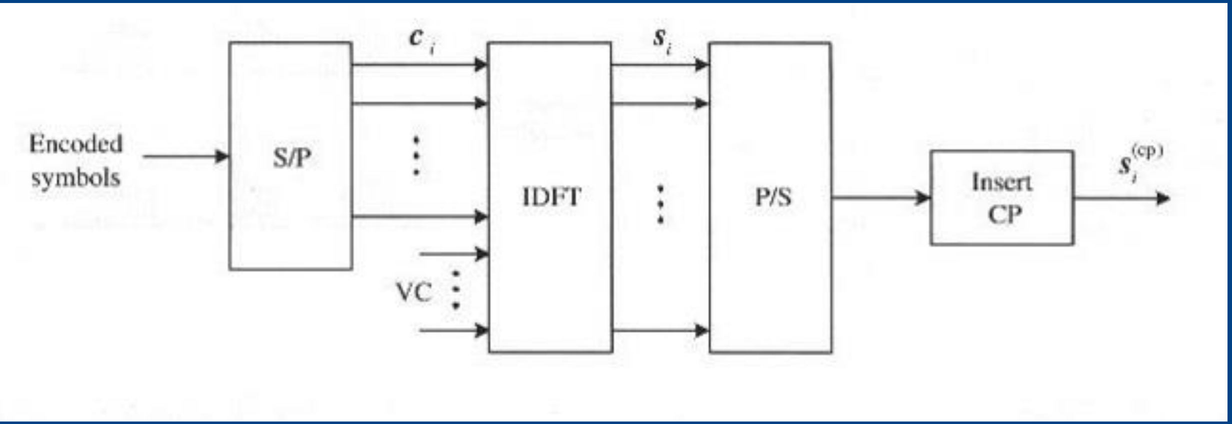

$$\boldsymbol{s}_i^{(cp)} = \boldsymbol{T}^{(cp)} \boldsymbol{s}_i \quad \boldsymbol{T}^{(cp)} = \begin{bmatrix} \boldsymbol{P}_{N_g \times N} \\ \boldsymbol{I}_N \end{bmatrix}$$

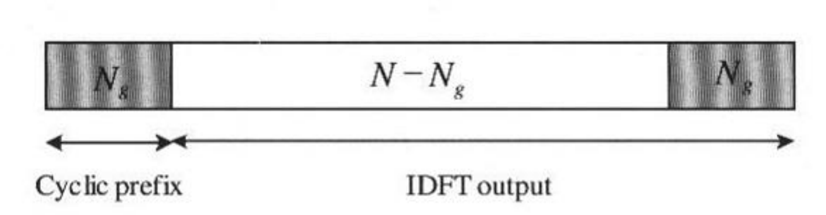

Dto. de Ingeniería Eléctrica y de Computadoras
Universidad Nacional del Sur

DIEC

OFDM discrete-time model (II)

After the channel ***h***, the received block is (not considering noise)

IBI !!

$$\boldsymbol{r}_i^{(cp)} = \boldsymbol{B}^l \boldsymbol{s}_i^{(cp)} + \boxed{\boldsymbol{B}^u \boldsymbol{s}_{i-1}^{(cp)}}$$

$$\boldsymbol{B}^l = \begin{bmatrix} h(0) & 0 & 0 & \cdots & 0 \\ h(1) & h(0) & 0 & \cdots & 0 \\ h(2) & h(1) & h(0) & \cdots & 0 \\ \vdots & \vdots & \vdots & \vdots & \vdots \\ h(L-1) & h(L-2) & h(L-3) & \cdots & 0 \\ 0 & h(L-1) & h(L-2) & \cdots & 0 \\ \vdots & \vdots & \vdots & \vdots & \vdots \\ 0 & 0 & \cdots & 0 & h(0) \end{bmatrix} \qquad \boldsymbol{B}^u = \begin{bmatrix} 0 & \cdots & 0 & h(1) & h(2) & \cdots & h(L-1) \\ 0 & \cdots & 0 & 0 & h(1) & \cdots & h(L-2) \\ \vdots & \vdots & \vdots & \ddots & \ddots & \ddots & \vdots \\ 0 & \cdots & \cdots & \cdots & \cdots & 0 & h(1) \\ 0 & \cdots & \cdots & \cdots & \cdots & \cdots & 0 \\ \vdots & \vdots & \vdots & \ddots & \ddots & \ddots & \vdots \\ 0 & \cdots & \cdots & \cdots & \cdots & \cdots & 0 \end{bmatrix}$$

If $h(n)$ is the channel impulse response of length *L*, to avoid IBI must be $N_g > L$

NEON

OFDM discrete-time model (III)

If the CP removal is performed by

$$\boldsymbol{R}^{(cp)} = \left[\begin{array}{cc} \boldsymbol{0}_{N\times N_g} & \boldsymbol{I}_N \end{array} \right]$$

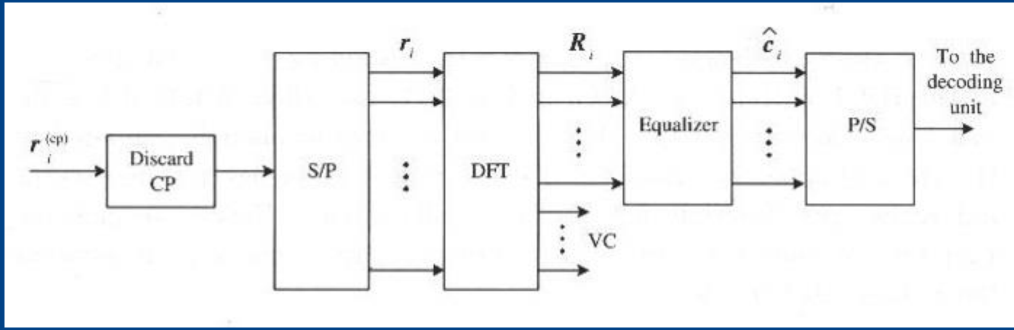

$$\boldsymbol{r}_i = \boldsymbol{R}^{(cp)}\boldsymbol{r}_i^{(cp)} = \left(\boldsymbol{R}^{(cp)}\boldsymbol{B}^l\boldsymbol{T}^{(cp)}\right)\boldsymbol{F}^H\boldsymbol{c}_i = \boldsymbol{B}_c\boldsymbol{F}^H\boldsymbol{c}_i$$

where, due to structure of the CP introduced, $\boldsymbol{B}_c$ is a ***circulant matrix***, that verifies

$$\boldsymbol{F}\boldsymbol{B}_c\boldsymbol{F}^H = \boldsymbol{D}_H$$

where $\boldsymbol{D}_H$ is diagonal with $\boldsymbol{H} = \sqrt{N}\boldsymbol{F}\boldsymbol{h}$ on its main diagonal.

OFDM discrete-time model (IV)

Hence,

$$\boldsymbol{R}_i = \boldsymbol{F}\boldsymbol{B}_c\boldsymbol{F}^H\boldsymbol{c}_i = \boldsymbol{D}_H\boldsymbol{c}_i$$

Or, in scalar form

$$R_i(n) = H(n)c_i(n),\ 0 \leq n \leq N-1$$

where

$$H(n) = \sum_{\ell=0}^{L-1} h(\ell)e^{-j2\pi n\ell/N}$$

is the channel frequency response.

OFDM discrete-time model (V)

Once again, after S/P and DFT, we obtain

$$\boldsymbol{R}_i = \boldsymbol{F}\boldsymbol{B}_c\boldsymbol{F}^H\boldsymbol{c}_i = \boldsymbol{D}_H\boldsymbol{c}_i$$

The data is recovered by

$$\hat{\boldsymbol{c}}_i = \boldsymbol{D}_H^{-1}\boldsymbol{R}_i$$

Since $\boldsymbol{D}_H$ is diagonal, above equation can be written in scalar form as

$$\hat{c}_i = \frac{R_i(n)}{H(n)},\ 0 \leq n \leq N-1$$

corresponding to a bank of one-tap equalizers $1/H(n)$

OFDM channel equalization basics

Assuming a channel static during the transmission of block i , but that can vary from block to block, the output of the DFT is

$$R_i(n) = H_i(n)c_i + W_i(n),\ 0 \leq n \leq N-1$$

For equalization purposes, in practice, we use $p_i(n)$ (known pilot symbol) and some specific design criterion.

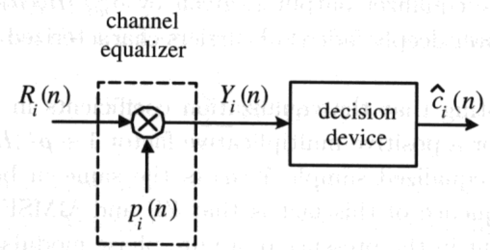

Fig. 4.1 Equalization and data detection over the nth subcarrier.

OFDM channel equalization basics (II)

Minimum mean-square error (MMSE) criterion

$$J_i(n) = E\{|p_i(n)R_i(n) - c_i|^2\}$$

From the orthogonality principle we know that

$$E\{[p_i(n)R_i(n) - c_i]R_i^*(n)\} = 0$$

Then, by computing the expectation with respect to the noise and data (assumed statistically independent with zero mean and bounded variance) we obtain

$$p_i(n) = \frac{H_i^*(n)}{|H_i(n)|^2 + 1/SNR}$$

OFDM channel equalization basics (III)

Zero-Forcing (ZF) criterion

Assuming no noise in previous model (or else $SNR \to \infty$)

$$p_i(n) = \frac{1}{H_i(n)}$$

while the DFT output takes the form

$$Y_i(n) = c_i(n) + \frac{W_i(n)}{H_i(n)}$$

that indicates that ZF equalization compensates any distortion induced by the channel. However, noise power at the equalizer output is increased.

OFDM channel estimation

Pilot-aided channel estimation

- Transmission of ODFM blocks is usually organized in a frame structure, with some reference known blocks at the beginning to assist the synchronization process. If the length of the frame is shorter than the coherence time, the channel remains constant during the transmission, and initial channel estimation is useful.

- If we consider a time varying scenario, channel change from block to block, and some additional information is required to perform equalization. To this purpose *pilots* are inserted into the payload section of the frame.

OFDM channel estimation (II)

- The pilots are scattered in both time and frequency directions (different blocks and different subcarriers), and are used as reference values for channel estimation and tracking.
- In practice, channel transfer function is first estimated at the positions where pilots are placed, and interpolation techniques are next employed to obtain the channel response over data subcarriers.
- Distribution of pilots in time and frequency depends, logically, on channel characteristics and application.

OFDM spectral efficiency

If compared with FDM (since overlapping is allowed by orthogonality), higher spectral efficiency is evident in OFDM.

Higher number of subcarriers in an specific bandwidth leads to even better results.

However, also leads to longer blocks that complicate synchronization and/or equalization due to time-selective fading.

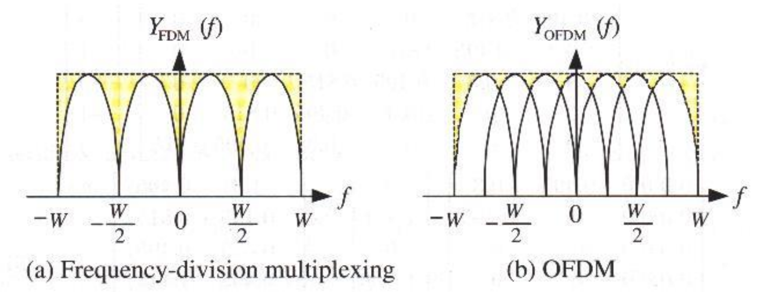

Fig. 2.19 Comparison between the spectral efficiencies of FDM and OFDM systems.

OFDM characteristics

Main advantages:

- Increased robustness against multipath fading
- High spectral efficiency due to partially overlapping subcarriers.
- Interference suppression capability through the use of cyclic prefix.
- Simple implementation by means of DFT/IDFT.
- Increased protection against narrowband interferences.
- Opportunity to use the subcarriers according to channel conditions.

Drawbacks:

- High sensitivity to frequency synchronization errors (stringent specifications for local oscillators).
- High Peak-to-Average Power Ratio (PAPR).
- Loss in spectral efficiency due to the use of the cyclic prefix.

OFDM based multiple access schemes

OFDM-TDMA: Not MAI if CP correctly designed. TDMA requires much higher instantaneous power than FDMA.

MC-CDMA: Diversity gain by SS, in addition to OFDM advantages. Frequency-selective channel introduces MAI since orthogonality between users is lost (sophisticated multi-user detection is required).

OFDMA: Assuming ideal synchronization, orthogonality is maintained, then MAI is avoided.

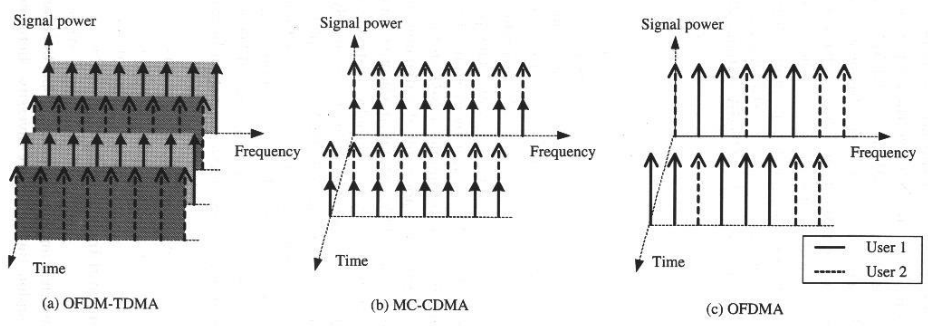

Fig. 2.20 Illustration of OFDM-based multiple-access schemes.

OFDM based multiple access schemes

Key drawback of OFDM signal for IoT

- High Peak-to-Average Power Ratio (PAPR): Addition of high number of subcarriers (modulated sinusoids) has almost Gaussian statistics.
- That requires high linearity (costly) power amplifier to reduce distortion.

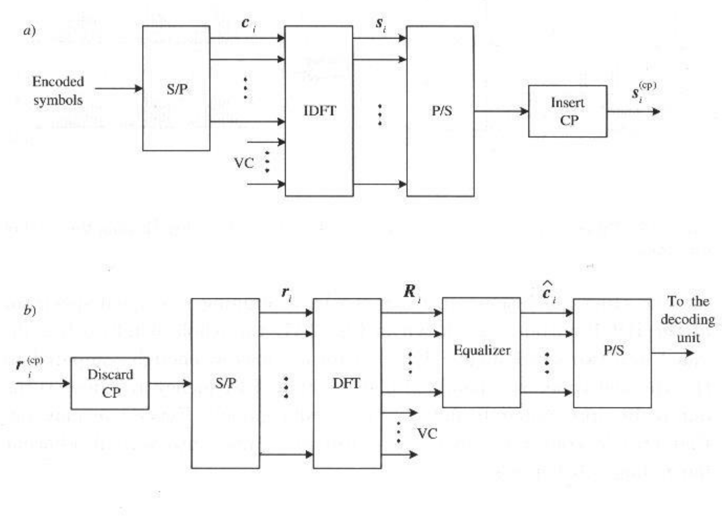

Fig. 2.15 Block diagram of a typical OFDM system: *a*) transmitter; *b*) receiver.

Not an issue in the downlink (base station to user) but problematic in the uplink.

OFDM based multiple access schemes

Alternative to OFDM:

Single Carrier – Frequency Domain Equalization (SC/FDE)

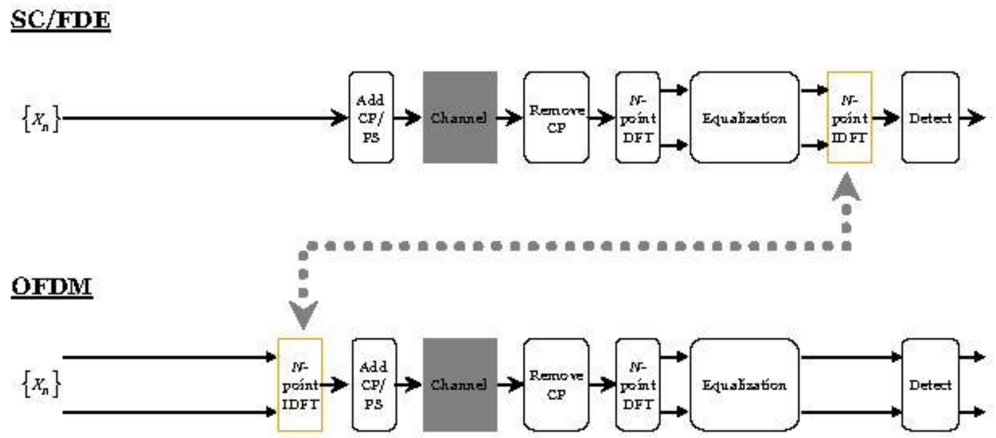

* CP: Cyclic Prefix, PS: Pulse Shaping

Figure 1 – SC/FDE and OFDM.

OFDM based multiple access schemes

Combination with OFDM for multiple users:

Single Carrier – Frequency Domain Multiple Access (SC-FDMA)

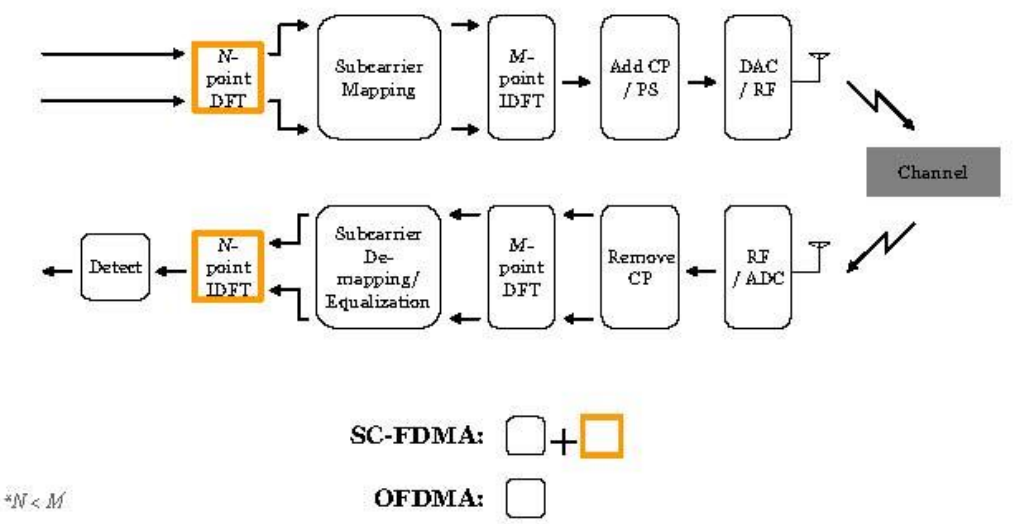

Figure 2 – A block diagram of an SC-FDMA system.

OFDM based multiple access schemes

Combination with OFDM for multiple users:

Single Carrier – Frequency Domain Multiple Access (SC-FDMA)

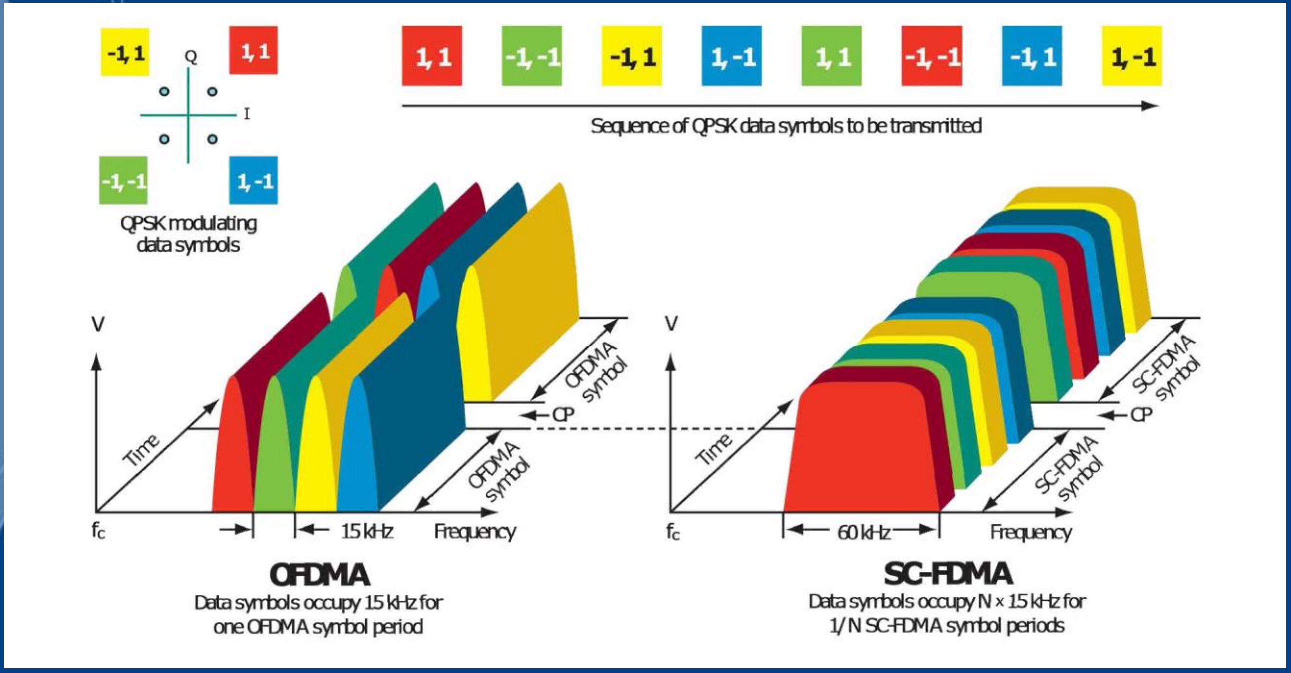

OFDM based multiple access schemes

SC – FDMA receiver details

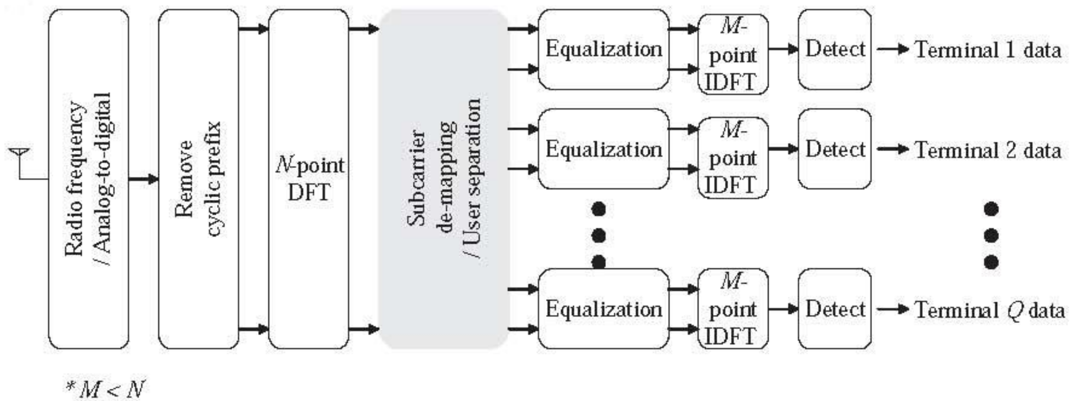

SC-FDMA receiver structure from a multiple user access perspective with $Q = N/M$ terminals in the uplink

It is evident that, in the same way that for OFDMA, user separation (in this case before FDE) is required.

OFDM Sensitivity to synchronization errors

- Timing synchronization, identification of the beginning of the block, or either the frame, to find the right position of the DFT window.
- Frequency synchronization, differences between carrier and local oscillator for demodulation results in a loss of orthogonality.
- Sampling clock synchronization, slightly different clocks at transmitter and receiver produces ICI. No practical effects in modern systems (solved by time synchronization).

OFDM Sensitivity… (II)

The time-domain samples of the *i-th* OFDM block are

$$s_i^{(cp)}(k) = \frac{1}{\sqrt{N}} \sum_{n \in \mathcal{I}} c_i(n) e^{j2\pi nk/N}, \qquad -N_g \leq k \leq N-1$$

and the equivalent baseband signal transmitted is given by

$$s_T(k) = \sum_i s_i(k - iN_T)$$

DIEC

OFDM Sensitivity… (III)

We define the difference between the local oscillator and the carrier frequency, normalized to the subcarrier, as the *normalized carrier frequency offset* (CFO),

$$f_d = f_c - f_{LO}, \qquad \epsilon = f_d/(1/NT_s)$$

and also θ is the time offset, i.e.: the number of samples by which the received time scale is shifted from its ideal setting. Then, the received signal is

$$r(k) = e^{j2\pi\epsilon k/N} \sum_i \sum_{l=0}^{L-1} h(l) s_i(k - \theta - l - iN_T) + w(k)$$

OFDM Sensitivity (IV)

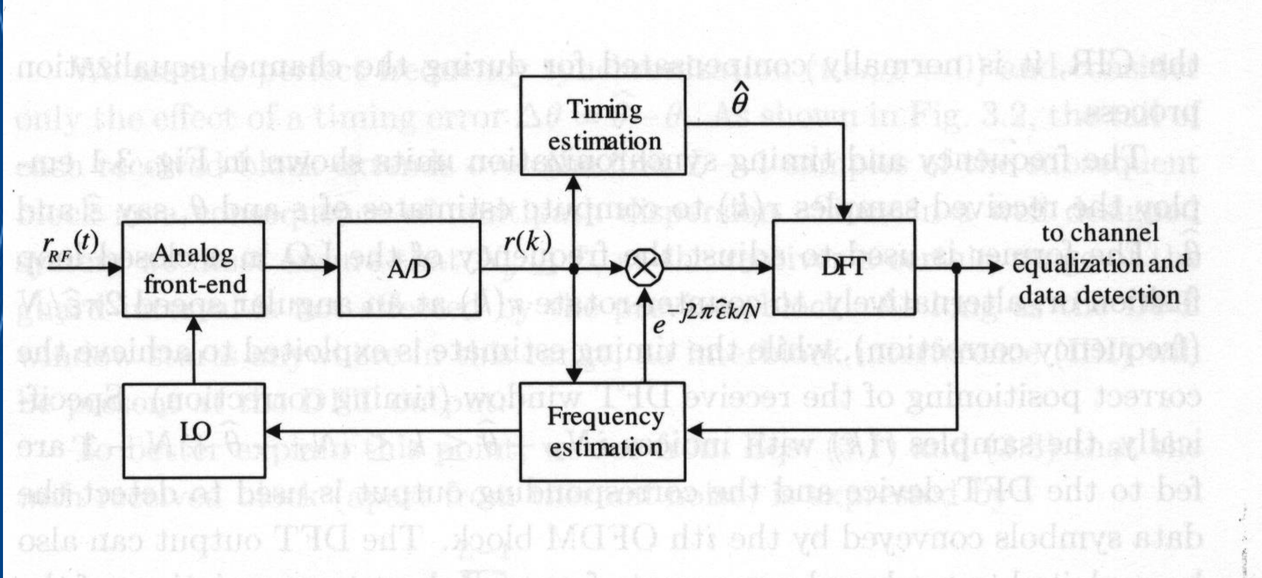

Fig. 3.1 Block diagram of an OFDM receiver.

Dto. de Ingeniería Eléctrica y de Computadoras
Universidad Nacional del Sur

DIEC

Timing offset effects (I)

Assuming perfect frequency synchronization and a well designed system, i.e. , $N_g \geq L$ then at the receiver a certain range of the guard interval is not affected by previous block. If the DFT starts anywhere in this range, no IBI will be present.

Defining $\Delta\theta = \hat{\theta} - \theta$ if

- $-N_g + (L-1) \leq \Delta\theta \leq 0$ no IBI!

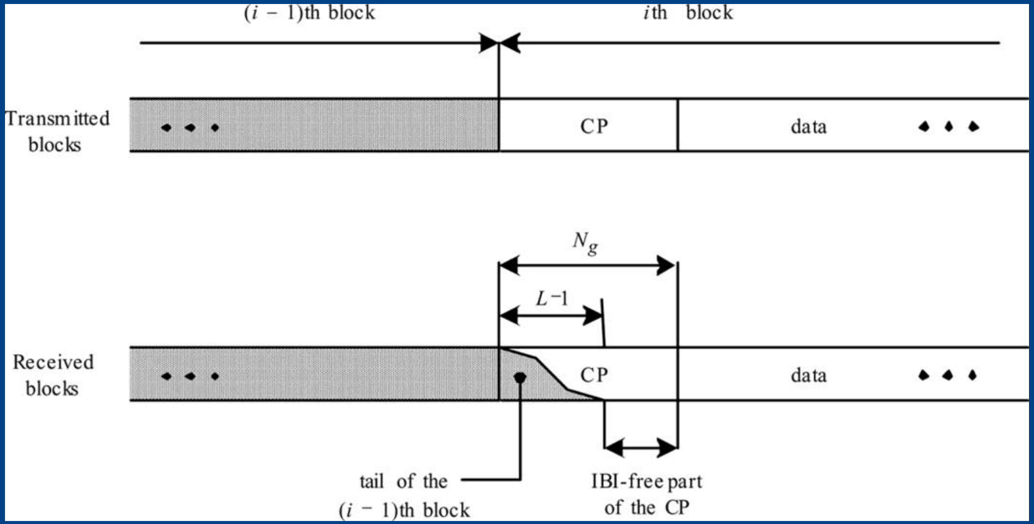

DIEC

Timing offset effects (II)

The DFT output over the *n-th* subcarrier can be represented by

$$R_i(n) = e^{j2\pi\Delta\theta/N} H(n) c_i(n) + W_i(n)$$

Since timing offset appears as a linear phase across the DFT outputs, it can be compensated by the channel equalizer.

This means that no single correct timing synchronization point exists in OFDM, since there are $N_g - L + 2$ of them.

DIEC

Timing offset effects (III)

If $N_g - (L-1) \leq \Delta\theta \quad \text{or} \quad \Delta\theta \geq 0$ there will be not only IBI but also loss of orthogonality among subcarriers, i.e., ICI.

Then, the n-th DFT output can be written as

$$R_i(n) = e^{j2\pi\Delta\theta/N}\alpha(\Delta\theta)H(n)c_i(n) + I_i(n,\Delta\theta) + W_i(n)$$

where $\alpha(\Delta\theta)$ is an attenuation factor and $I_i(n,\Delta\theta)$ reflects IBI and ICI that can be modeled as zero-mean random variable with power $\sigma_I^2(\Delta\theta)$.

Timing offset effects (IV)

An indicator to evaluate the effects of timing error is the *loss in SNR*, as defined by

$$\gamma(\Delta\theta) = \frac{SNR^{ideal}}{SNR^{real}}$$

After some elaboration:

$$\gamma(\Delta\theta) = \frac{1}{\alpha^2(\Delta\theta)}\left(1 + \frac{\sigma_I^2(\Delta\theta)}{\sigma_w^2}\right)$$

Dto. de Ingeniería Eléctrica y de Computadoras
Universidad Nacional del Sur

DIEC

Timing offset effects (V)

Example:

N= 256, N_g=16.

Rayleigh fading channel with *L=8* and exponentially decaying power delay profile.

For a given timing error SNR loss increases with E_s/N_0 (at low SNR the main impairment is thermal noise).

To keep SNR loss tolerable (less than *1 dB*) residual error after timing correction should be a small percentage of *N*.

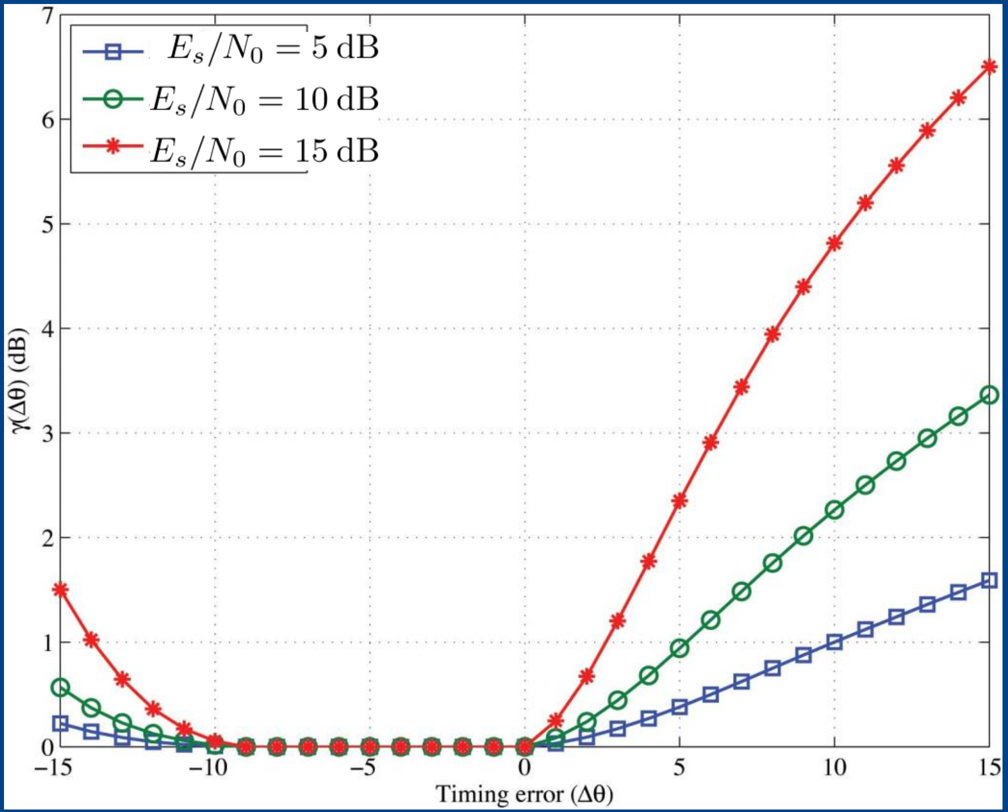

NEON

DIEC

Frequency offset effects (I)

Assuming now perfect timing synchronization, at the receiver DFT output the *i-th* OFDM block can be written as

$$R_i(n) = e^{j\varphi_i} \sum_{m \in \mathcal{I}} H(m) c_i(m) e^{j\pi(N-1)(\epsilon+m-n)/N} f_N(\epsilon + m - n) + W_i(n)$$

$$f_N(x) = \frac{\sin(\pi x)}{N \sin(\pi x / N)} \qquad \varphi_i = 2\pi i \epsilon N_T / N$$

DIEC

Frequency offset effects (II)

Considering the case in which the frequency offset is a *multiple* of the subcarrier spacing 1/NT, then

$$R_i(n) = e^{j\varphi_i} H(|n-\epsilon|_N) c_i(|n-\epsilon|_N) + W_i(n)$$

then orthogonality is not destroyed and that frequency offset only results into a shift of the subcarrier indices.

Frequency offset effects (III)

For the case in which the frequency offset is a fraction of the subcarrier spacing, then

$$R_i(n) = e^{j[\varphi_i + \pi\epsilon(N-1)/N]} H(n) c_i(n) f_N(\epsilon) + I_i(n,\epsilon) + W_i(n)$$

where $I_i(n,\epsilon)$ accounts for ICI.

Letting $E\{|H(n)|^2\} = 1$ as before, and assuming *i.i.d.* data symbols with zero mean and power E_s, the ICI term has zero mean and its power can be written as

$$\sigma_I^2(\epsilon) = E_s(1 - f_N^2(\epsilon))$$

Frequency offset effects (IV)

Using the SNR loss to study the impact of the frequency errors, the following results can be obtained

$$\gamma(\epsilon) = \frac{SNR^{ideal}}{SNR^{real}} \qquad \gamma(\epsilon) = \frac{1}{f_N^2(\epsilon)}\left(1 + \frac{E_s}{N_0}(1 - f_N^2(\epsilon))\right)$$

That, for small values of the frequency offset, can be approximated to

$$\gamma(\epsilon) \cong 1 + \frac{1}{3}\frac{E_s}{N_0}(\pi\epsilon)^2$$

Frequency offset effects (V)

Example:

Same OFDM and channel parameters than in previous example.

To avoid severe degradation frequency offset should be as low as 4-5 % of subcarrier spacing.

For example with 1/NT = 15 kHz, then a tolerable freq. offset 500 Hz. For a carrier = 5 GHz, this corresponds to an oscillator instability of 0.3 ppm. For practical designs (low cost approx. 20 ppm) this requires frequency offset estimation and correction.

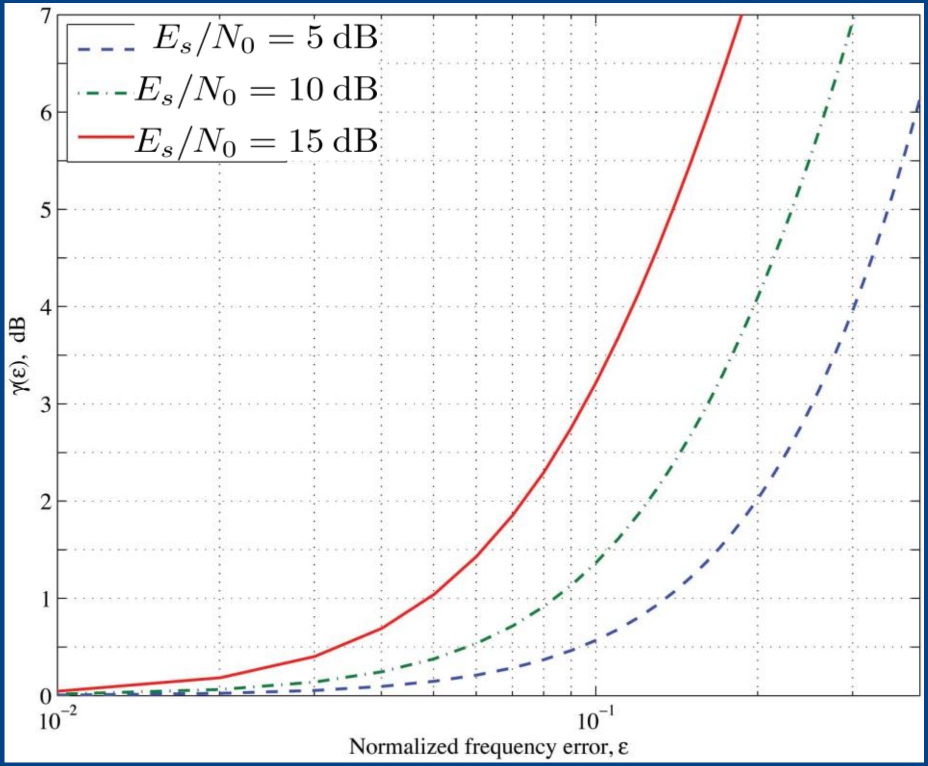

DIEC

Conclusions

- OFDM concept introduce considerable simplifications in terms of equalization of frequency selective channels.

- Sensitivity of OFDM to timing and frequency offset errors must be counteracted in any practical implementation.

- Timing errors can be reduced with proper design of the cyclic prefix.

- Only small carrier frequency offset can be tolerated if ICI is expected not to affect BER performance in OFDM.

DIEC

Downlink time and CFO synchronization

1. OFDMA transmitter – Downlink synchronization tasks
2. Downlink acquisition (coarse synchronization)
3. Downlink tracking (fine synchronization)

Downlink synchronization tasks (I)

- Similar tasks that performed with conventional single-user OFDM.
- MU uses the broadcast signal transmitted by BS to get timing and frequency estimates, that will be used to control the position of the DFT window and the frequency of the local oscillator.
- Synchronization process is split into an acquisition step followed by a tracking phase.

Downlink synchronization tasks (II)

- *Acquisition process*: pilot blocks with a particular repetitive structure are used to get initial estimates of the synchronization parameters. Specific algorithms must cope with large errors. Phases: frame detection, timing and CFO estimation.

- *Tracking process*: Devoted to maintain and/or refine initial timing and frequency estimates, and also counteract small short-term variations due to oscillator drifts and Doppler shifts.

Downlink synchronization tasks (III)

Simplified frame structure includes:

- Null block (no signal), at the beginning, to estimate interference and noise power.
- Reference blocks, known structure and/or symbols (acquisition tasks).
- Pilot tones: subcarriers with known symbols (tracking tasks).

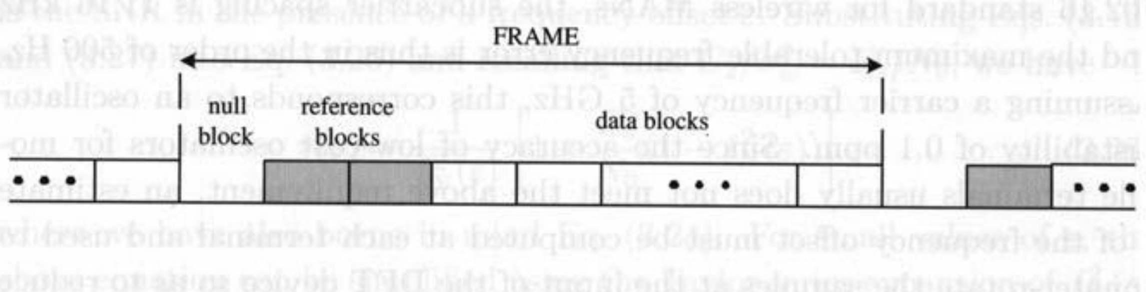

Fig. 3.5 Example of frame structure in the downlink.

Downlink synchronization tasks (IV)

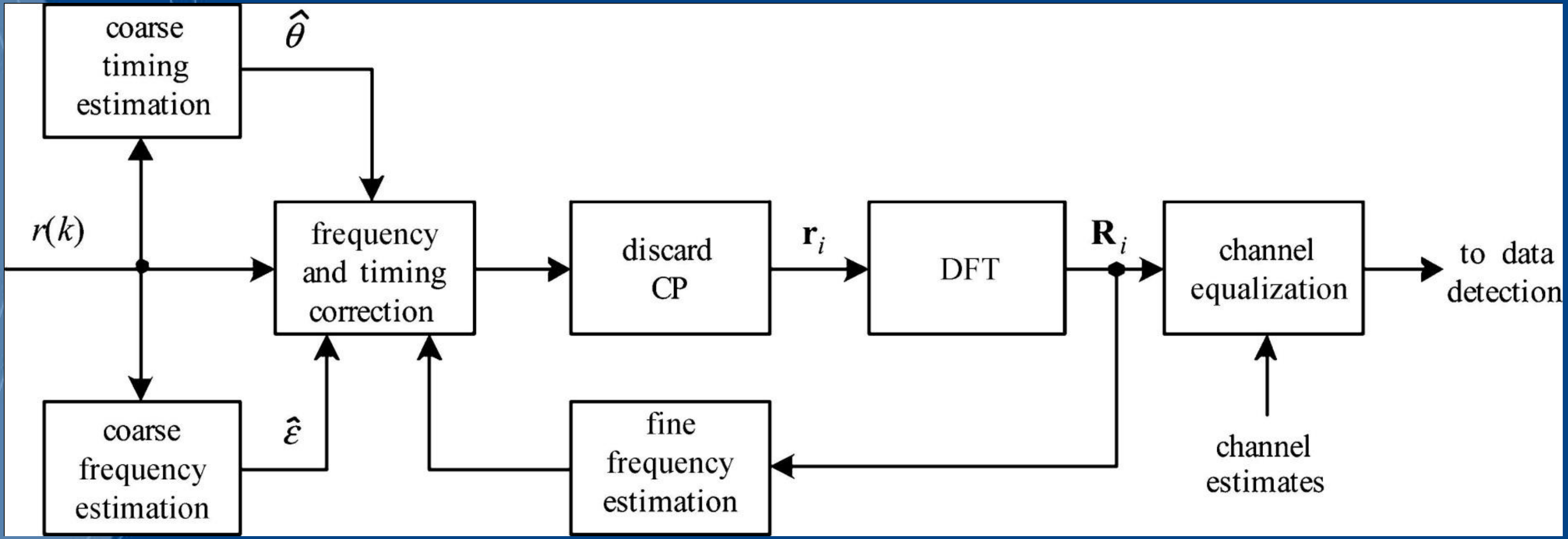

Block diagram of OFDMA downlink receiver

Downlink timing acquisition

Schmidt and Cox algorithm: Use of reference block with two identical halves (in time domain). This can be generated, in the frequency domain, modulating only subcarriers with even indices with a PN sequence $\boldsymbol{c} = [c(0), c(2), \cdots, c(N-2)]^T$, and setting to 0 the subcarriers with odd indices.

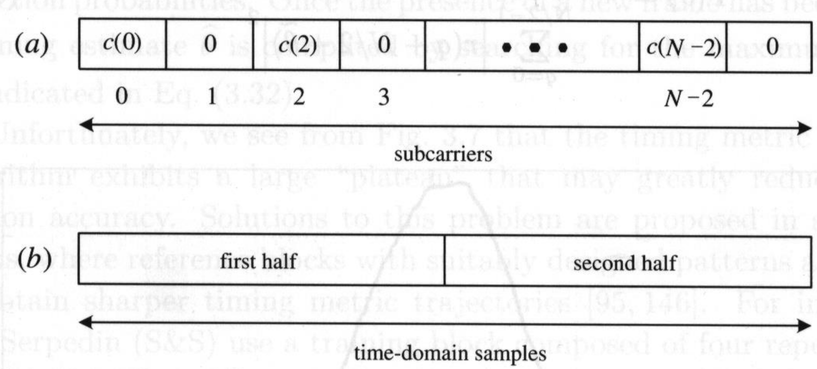

Fig. 3.6 S&C reference block in the frequency-domain (a) and in the time-domain (b)

Downlink timing acquisition (II)

If the CP is properly designed, both halves remain identical after passing through the channel except for a phase difference caused by the CFO. Hence,

$$r(k) = s_R(k)e^{j2\pi\epsilon k/N} + w(k), \qquad \theta \leq k \leq \theta + N/2 - 1$$

$$r(k+N/2) = s_R(k)e^{j2\pi\epsilon k/N}e^{j\pi\epsilon} + w(k+N/2), \qquad \theta \leq k \leq \theta + N/2 - 1$$

Dto. de Ingeniería Eléctrica y de Computadoras
Universidad Nacional del Sur

DIEC

Downlink timing acquisition (III)

Then, the magnitude of a sliding window correlation of lag N/2 gives a peak when the window is aligned with the reference block

$$\hat{\theta} = \arg\max_{\hat{\theta}}\{|\Gamma(\tilde{\theta})|\} \qquad \Gamma(\hat{\theta}) = \frac{\sum_{q=0}^{N/2-1} r(q+N/2+\tilde{\theta})r^*(q+\tilde{\theta})}{\sum_{q=0}^{N/2-1} \left|r(q+N/2+\tilde{\theta})\right|^2}$$

For frame detection, $|\Gamma(\tilde{\theta})|$ is compared against a given threshold λ, designed to achieve a reasonable trade-off between false alarm and misdetection probabilities.

Downlink timing acquisition (IV)

Example: Obtained with *N*=256, *Ng*=16, Rayleigh multipath channel, *L*=8 and *SNR*= 20 dB.

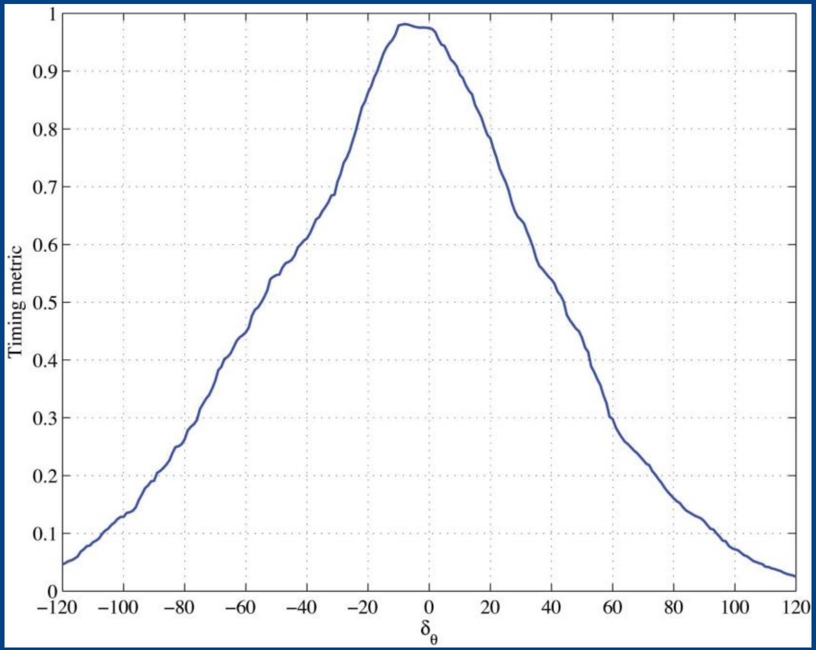

Timing metric of S-C algorithm exhibits considerable ambiguity that reduce the estimation accuracy.

Downlink timing acquisition (V)

S-S algorithm: Use of a training block composed of 4 repetitive parts, defined by: $[+B \ \ +B \ \ -B \ \ +B]$

A sliding window spans the received time-domain samples with indices $\tilde{\theta} \leq k \leq \tilde{\theta} + N - 1$, that defines 4 vectors

$$\boldsymbol{r}_j = \{r(k + jN/4 + \tilde{\theta}); 0 \leq N/4 - 1\}, \qquad \text{with } j = 0, 1, 2, 3$$

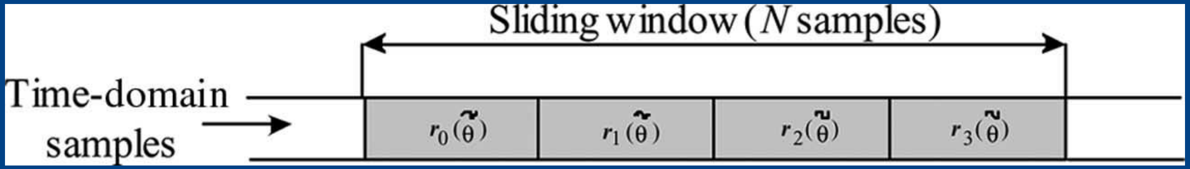

Downlink timing acquisition (VI)

Timing metric of SS algorithm is computed as

$$\Gamma_{SS}(\hat{\theta}) = \frac{|\Lambda_1(\tilde{\theta})| + |\Lambda_2(\tilde{\theta})| + |\Lambda_3(\tilde{\theta})|}{\frac{3}{2}\sum_{j=0}^{3}\left\|\boldsymbol{r}_j(\tilde{\theta})\right\|^2}$$

where

$$\begin{aligned}
\Lambda_1(\tilde{\theta}) &= \boldsymbol{r}_0^H(\tilde{\theta})\boldsymbol{r}_1(\tilde{\theta}) - \boldsymbol{r}_1^H(\tilde{\theta})\boldsymbol{r}_2(\tilde{\theta}) - \boldsymbol{r}_2^H(\tilde{\theta})\boldsymbol{r}_3(\tilde{\theta}) \\
\Lambda_2(\tilde{\theta}) &= \boldsymbol{r}_1^H(\tilde{\theta})\boldsymbol{r}_3(\tilde{\theta}) - \boldsymbol{r}_0^H(\tilde{\theta})\boldsymbol{r}_2(\tilde{\theta}) \\
\Lambda_3(\tilde{\theta}) &= \boldsymbol{r}_0^H(\tilde{\theta})\boldsymbol{r}_3(\tilde{\theta})
\end{aligned}$$

Downlink timing acquisition (VII)

Example: Similar to previous example.

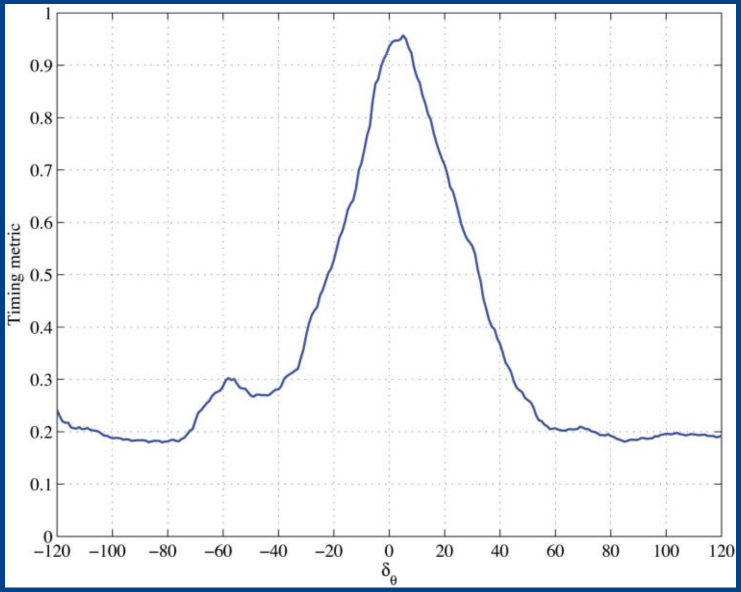

Downlink Frequency acquisition

Moose algorithm: assuming time acquisition has been achieved, let $R_1(n)$ and $R_2(n)$ be the *n*th DFT output corresponding to the two reference blocks. Then,

$$R_1(n) = S_R(n) + W_1(n) \qquad R_2(n) = S_R(n)e^{j2\pi\epsilon N_T/N} + W_2(n)$$

An estimate of the CFO is

$$\hat{\epsilon} = \frac{1}{2\pi(N_T/N)} \arg\left\{\sum_{n=0}^{N-1} R_2(n)R_1^*(n)\right\}$$

Main drawback: short acquisition range. Since $\arg\{.\}$ return values in $[-\pi, \pi)$, then is must be

$$|\hat{\epsilon}| \leq N/(2N_T)$$

Downlink Frequency acquisition (II)

S-C algorithm: Uses also 2 reference blocks, but with the following structure

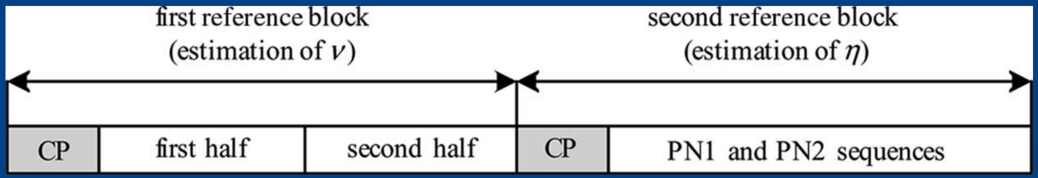

First block the same used for timing acquisition. 2nd block contains a differentially encoded PN1 on even subcarriers and another PN2 on odd subcarriers.

DIEC

Downlink Frequency acquisition (III)

Assuming timing acquisition done, with θ successfully estimated, frequency error is decomposed into a fractional part (less than *1/T* in magnitude) and an integer part (multiple of *2/T*), with *T* = *NTs*.

Then the normalized CFO can be written as

$$\epsilon = \nu + 2\eta \qquad \nu \in (-1, 1], \text{and } \eta \text{ is an integer.}$$

S-C algorithm uses the first reference block to estimate the fractional part as

$$\hat{\nu} = \frac{1}{\pi} \arg \left\{ \sum_{k=\theta}^{\theta+N/2-1} r(k+N/2) r^*(k) \right\}$$

Dto. de Ingeniería Eléctrica y de Computadoras
Universidad Nacional del Sur

DIEC

Downlink Frequency acquisition (IV)

Fractional CFO estimate is compensated (counter- rotating the time domain samples) and fed to DFT unit.

If $R_1(n)$ and $R_2(n)$ are the DFT of first and 2nd block, DFT outputs will be shifted from their correct position if $\eta \neq 0$ (remember frequency effects of CFO), i.e.,

$$R_1(n) = e^{j\varphi_1} H(|n - 2\eta|_N) c_1(|n - 2\eta|_N) + W_1(n)$$

$$R_2(n) = e^{j(\varphi_1 + 4\pi\eta N_T/N)} H(|n - 2\eta|_N) c_2(|n - 2\eta|_N) + W_2(n)$$

NEON

Downlink Frequency acquisition (V)

Neglecting noise terms, and defining $d(n) = c_2(n)/c_1(n)$, it is possible to conclude that, for *n* even

$$R_2(n) \cong e^{j4\pi\eta N_T/N} d(|n - 2\eta|_N) R_1(n)$$

Then, an estimate of η can be obtained by looking for the integer that maximizes

$$B(\tilde{\eta}) = \frac{\left|\sum_{n\in J} R_2(n) R_1^*(n) d(|n - 2\eta|_N)\right|}{\sum_{n\in J} |R_2(n)|^2}$$

where *J* is the set of indices for the even subcarriers.

DIEC

Downlink Frequency acquisition (VI)

Final CFO estimation of the S-C algorithm is given by

$$\hat{\epsilon} = \hat{\nu} + 2\hat{\eta}$$

Its MSE can be approximated by

$$MSE\{\hat{\epsilon}\} = \frac{2(SNR)^{-1}}{\pi^2 N}$$

DIEC

Downlink Frequency acquisition (VII)

M-M algorithm: extension of S-C algorithm, by considering a reference block composed by $Q \geq 2$ repetitive parts, each comprising $P = N/Q$ time domain samples. The estimated CFO is

$$\hat{\epsilon} = \frac{Q}{2\pi} \sum_{q=1}^{Q/2} \xi(q) \arg\left\{ \Psi(q) \Psi(q-1) \right\}$$

$$\Psi(q) = \sum_{k=\theta}^{\theta+N-qP-1} r(k+qP) r^*(k), \quad q = 1, 2, \cdots, Q/2$$

$$\xi(q) = \frac{12(Q-q)(Q-q+1) - Q^2}{2Q(Q^2-1)}$$

DIEC

Downlink Frequency acquisition (VIII)

If *Q* is designed such that CFO is in $[-Q/2, Q/2]$, the M-M algorithm gives a CFO estimate that not requires a 2nd reference block.

The MSE of the estimate is given by

$$MSE\{\hat{\epsilon}\} = \frac{3(SNR)^{-1}}{2\pi^2 N(1-1/Q^2)}$$

lower than that of the S-C algorithm for $Q > 2$.

Downlink timing tracking

- Non negligible errors in the sampling clock frequency (due to clock oscillators) should result in a short–term variation of the timing error $\Delta\theta$ which must be tracked.

- Basic solution: associate $\Delta\theta$ as introduced by the channel rather than oscillator drift, that means to replace $\boldsymbol{h} = [h(0), h(1), \cdots, h(L-1)]^T$ by

$$\boldsymbol{h}'(\Delta\theta) = [h(\Delta\theta), h(1+\Delta\theta), \cdots, h(L-1+\Delta\theta)]^T$$

Then, channel estimates over different blocks are differently delayed.

To track these fluctuations look for the delay of the first significant tap of the estimated CSI. The integer part of this delay is used to control DFT window, and the fractional part is compensated be the channel equalizer.

Downlink timing tracking (II)

A CP-based timing tracking scheme: The following time metric is used

$$\gamma(k) = \sum_{k=0}^{N_g-1} r(k+q)r^*(k-q-N), \quad k \text{ current received sample}$$

Since the CP introduces periodicity due to the identically repeated *Ng* samples of each block, $\gamma(k)$ will exhibit peaks

Downlink timing tracking (III)

Example: N= 256, Ng=16. Rayleigh multipath channel with L=8 taps.

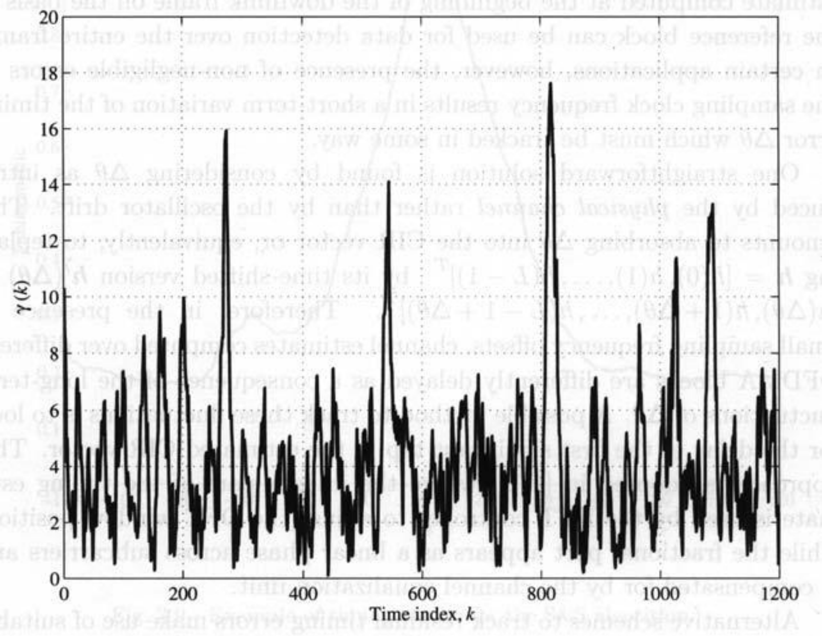

A remedy to have more robust results against interference and noise is to introduce the following smoother to the obtained estimate

$$\bar{\gamma}(k) = \alpha\bar{\gamma}(k - N_T)(1-\alpha)\gamma(k)$$

where $0 < \alpha \leq 1$ must chosen to tradeoff between estimation accuracy and tracking capabilities.

Downlink frequency tracking

CFO estimate obtained during the acquisition phase is used to adjust the LO to produce new received samples

$$r'(k) = r(k)e^{-j2\pi k\hat{\epsilon}/N}$$

Since $r'(k)$ may still be affected by a residual frequency error $\Delta\epsilon = \epsilon - \hat{\epsilon}$ a non-negligible ICI will be present at DFT output.

In such conditions, tracking becomes necessary.

Downlink frequency tracking (II)

A general close-loop scheme for frequency tracking uses $r'(m)$ $(-N_g \leq m \leq N-1)$ to obtain corrected $R_i(n)$, and time or frequency strategies to define e_i , the error proportional to the residual CFO.

For each new received block

$$\Delta\hat{\epsilon}_{i+1} = \Delta\hat{\epsilon}_i + \alpha e_i$$

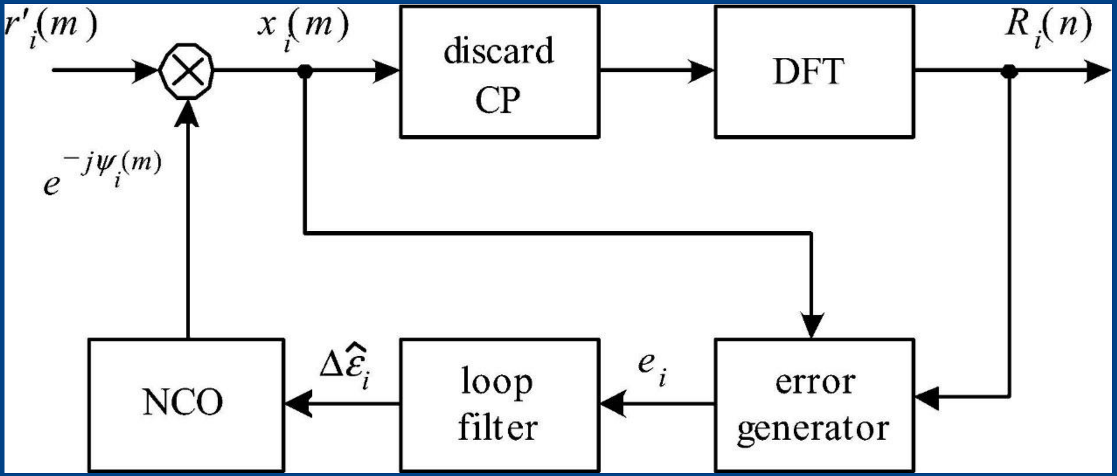

DIEC

Downlink frequency tracking (III)

The corrective phase is computed recursively as

$$\psi_i(m) = \psi_i(m-1) + 2\pi\Delta\hat{\epsilon}_i/N, \; -N_g \leq m \leq N$$

where $\psi_i(-N_g - 1)$ is set equal to $\psi_{i-1}(N-1)$ to avoid any phase jump between the last and first samples of blocks (*i-1*) and *i*.

Depending on whether e_i is obtained using $R_i(n)$ or $x_i(m)$ it is possible to consider different solutions.

Downlink frequency tracking (IV)

Time domain scheme: Uses the redundancy offered by the CP to obtain

$$e_i = \frac{1}{N_g} Im \left\{ \sum_{m=-N_g}^{-1} x_i(m+N) x_i^*(m) \right\}$$

A small perturbation analysis is useful to obtain an interpretation. Without any interference, the presence of a residual frequency offset leads to

$$x_i(n+N) \cong x_i(n) e^{j2\pi(\Delta\epsilon - \Delta\hat{\epsilon}_i)}, \ -N_g \leq m \leq -1$$

that means, $e_i \cong K \sin[2\pi(\Delta\epsilon - \Delta\hat{\epsilon}_i)]$ Note that the sign of $(\Delta\epsilon - \Delta\hat{\epsilon}_i)$ defines that of e_i , and then a decrement or increment of $\Delta\hat{\epsilon}_{i+1}$, where the equilibrium point is $\Delta\hat{\epsilon}_{i+1} = \Delta\hat{\epsilon}_i$

Downlink frequency tracking (V)

Frequency domain approach: a basic scheme, based on ML, uses

$$e_i = Re\left\{\sum_{n\in\mathcal{I}} R_i^*(n)[R_i(n+1) - R_i(n-1)]\right\}$$

An improved variant considers

$$e_i = Re\left\{\sum_{n\in\mathcal{I}} \frac{R_i^*(n)[R_i(n+1) - R_i(n-1)]}{1+\beta|R_i(n)|^2}\right\}$$

where β depends on the operating SNR.

DIEC

Conclusions

- In a general time varying frame context (i.e., time varying during the frame length), synchronization is divided in acquisition and tracking.
- Timing acquisition and tracking can be performed based on basic cross-correlation techniques.
- Carrier frequency offset estimation methods analyzed (all use training sequences) have different range (if related to subcarrier separation), with some advantage for those that not require the estimation of the CFO integer part.